BIOACTIVE COMPOUNDS OF *Moringa oleifera* AS KRAS^{G12C} INHIBITORS IN COLORECTAL CANCER: IN SILICO STUDY

Sephia Tiara Marviella*, Salma Zulqaida, Theresia Indah Budhy Sulisetyawati, Anwar Ma'ruf
Master of Immunology, Postgraduate School, Universitas Airlangga, Jl. Airlangga No. 4-6, Surabaya 60286, East Java, Indonesia
*Email: sephia.tiara.marviella-2022@pasca.unair.ac.id

Received 05 September 2024
Accepted 19 November 2024

Abstract

KRAS is a GTPase enzyme that regulates cell growth and division. Mutations in KRAS can lead to its permanent activation, resulting in uncontrolled cell growth and cancer progression. Approximately 30–44% of colorectal cancer cases harbor KRAS mutations, with 1–3% involving the KRAS^{G12C} variant. Historically considered "undruggable," recent advancements, such as Sotorasib, have demonstrated the potential to target KRAS^{G12C} effectively, making it a promising focus for drug discovery. *Moringa oleifera*, a plant rich in phytochemicals, is a potential source of bioactive compounds with therapeutic applications. In this study, 218 compounds derived from *M. oleifera* were screened using molecular docking, targeting KRAS^{G12C}. Quercetin (**3**) exhibited the lowest binding affinity (-9.37 kcal/mol) and showed interactions with key residues, including GLN100A, VAL104A, LYS17A, and TYR97A, suggesting a binding mechanism similar to that of Sotorasib as native ligand. The physicochemical analysis further revealed high gastrointestinal absorption, good lipophilicity, and favorable bioavailability scores for Quercetin (**3**), supporting its potential as a drug candidate. These findings highlight the potential of *M. oleifera* compounds, particularly quercetin (**3**), as inhibitors of KRAS^{G12C} in colorectal cancer.

Keywords*: colorectal cancer, KRAS^{G12C}, molecular docking, Moringa oleifera*

Introduction

Cancer remains a leading cause of death worldwide, with colorectal cancer ranking as the second most common cancer-related death (904,019) and the third most common cancer by incidence at 1.9 million worldwide in 2022 (Ferlay *et al*., 2021). In Indonesia, colorectal cancer ranked fourth in incidence, with 35,676 cases and 19,255 deaths reported in 2022 (Ferlay *et al*., 2021). Colorectal cancer can be caused by mutations in key genes that regulate cell division and growth, most notably the Kirsten Sarcoma (KRAS) gene.

KRAS protein is a GTPase (guanosine triphosphatase) that has a role as a molecular switch. It regulates signals for the promotion of cell growth and division (Simanshu *et al*., 2017). KRAS is bound to GDP in its inactive state and will bind to GTP during signal activation. The process will activate crucial signaling pathways, such as the MAPK (mitogen-activated protein kinase), for cellular proliferation and survival (Cully and Downward, 2008; Hobbs *et al*., 2016; Milburn *et al*., 1990). In cancer, this process is frequently dysregulated. KRAS mutations occur in approximately 30-44% of colorectal cancer, with 1-3% of mutation mutations affecting the KRAS^{G12C} (glycine at position 12 is replaced by cysteine) (Giannakis *et al*., 2016; Neumann *et al*., 2009; Parikh *et al*., 2022; Yaeger *et al*., 2018). The mutation locks KRAS in the GTP-bound state, which causes it to be permanently active.

In this state, cell growth cannot be controlled and will lead to cancer progression (Parikh *et al*., 2022).

For many years, the KRAS protein was considered an impossible drug target. This is caused by several reasons including its structural properties, rapid cycling between active and inactive states, and also the absence of well-defined druggable pockets (Huang *et al*., 2021). However, in 2013, it was found that KRAS is a viable drug target. Currently, drugs such as Sotorasib (AMG-510) and Adagrasib (MRTX849) have been clinically approved to target the $KRAS^{G12C}$ mutation, the structure has shown in Figure 1. (Ostrem *et al*., 2013; Canon *et al*., 2019; Jänne *et al*., 2022). This makes KRAS an interesting protein to be explored as a potential target for developing new drugs with natural products like *M. oleifera*.

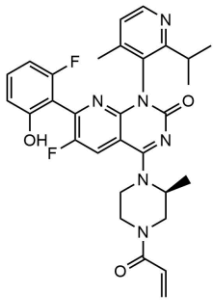

Sotorasib (**1**)

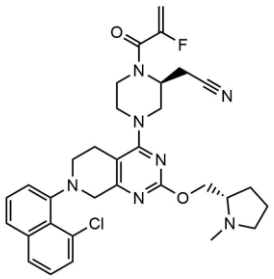

Adagrasib (**2**)

Figure 1. The structure of Sotorasib (**1**) and Adagrasib (**2**)

Moringa oleifera is a plant rich in secondary metabolites. It is abundant with phytochemicals, such as flavonoids (Lin *et al*., 2018), alkaloids (Sahakitpichan *et al*., 2011; Xie *et al*., 2021), saponin (Sharma and Paliwal, 2014), tannin, and isothiocyanate (Waterman *et al*., 2014) and some of these compounds have been reported to possess various biological activities, including antioxidant (Tukiran *et al*., 2020), anti-inflammatory, antidiabetic, and anticancer properties (Mthiyane *et al*., 2022). The in silico study of *Moringa oleifera* also demonstrated its potential anticancer activity through the inhibition of the BAX protein. Quercetin, identified as the active compound, showed a strong binding affinity to the target protein (Mumtaz *et al*., 2021). These findings suggest that *Moringa oleifera* is a promising and interesting source for the development of novel therapeutic agents

From the various phytochemical compounds reported in *M. oleif*era (Aja *et al*., 2021; Kashyap *et al*., 2022; Sivani *et al*., 2021; Teclegeorgish *et al*., 2021), it is hypothesized that some of these compounds may have the potential of novel therapeutic agents to inhibit the $KRAS^{G12C}$ mutation in colorectal cancer as well. To explore this possibility, structure-based virtual screening has been used. This computational technique allows for the rapid scanning of a library of small compounds by docking them into the binding pocket of a protein or enzyme, differentiating between predicted active and inactive compounds (Kontoyianni, 2017). Therefore, this study aims to evaluate the binding affinity and potential inhibitory effects of *Moringa oleifera* compounds on the KRASG12C protein using virtual screening, with the goal of identifying potential new drug candidates for colorectal cancer.

Research Methods

Ligand library preparation (datasets)

A total of 218 compounds derived from *M. oleifera* were selected for virtual screening. Of these, 169 compounds were

retrieved from the Natural Product Activity and Species Source Database (NPASS) (Zhao *et al*., 2023) while the remaining 49 compounds were sourced by additional literature (Aja *et al*., 2021; Kashyap *et al*., 2022; Sivani *et al*., 2021; Teclegeorgish *et al*., 2021). The Simplified Molecular-Input Line-Entry System (SMILES) format of the compounds was compiled to create the ligand library. The screening of drug-like and lead-like properties was performed using OpenBabel, applying Lipinski's Rule of Five (Ro5) alongside Ghose and Veber filters (Castro-González *et al*., 2020; O'Boyle *et al*., 2011). The screened compounds were then converted into a three-dimensional structure using the Balloon software (Puranen *et al*., 2010). Afterward, the structures were protonated at physiological pH (7.4), and geometrically optimized using the MMFF94 force field in the OpenBabel program.

Molecular docking for native ligand

The structure of the protein target, human $KRAS^{G12C}$, bound to the native ligand Sotorasib (AMG 510), was obtained from the RCSB Protein Data Bank (PDB: 6OIM) (Canon *et al*., 2019). For docking analysis, the Sotorasib structure was modified to its original state before it was formed a covalent bond with cysteine-12. The protein target and native ligand were prepared using the DockPrep tools in UCSF Chimera ver. 1.17.3 (Pettersen *et al*., 2004). The redocking procedure between the target protein and native ligand was carried out using the SMINA software (Koes *et al*., 2013). The DockRMSD program (Bell and Zhang, 2019) was used to calculate the RMSD value, the docking parameter was considered valid when the RMSD value is ≤ 2.0 Å. (Da Fonseca *et al*., 2024). The docking parameters were then used for virtual screening.

Molecular docking and virtual screening

The virtual screening between the *M. oleifera* compounds library and the prepared protein target was carried out by the SMINA software using the optimized docking parameter (Koes *et al*., 2013). The docking results were then ranked by the top ten highest affinity values using the sdsorter program.

Visualization, interaction analysis, and physicochemical properties prediction

The docking results were analyzed and visualized by the Protein-Ligand Interaction Profiler (PLIP) website (https://plip-tool.biotec.tu-dresden.de/plip-web/plip/index) and PyMOL ver. 2.5.4 (Schrodinger, 2015) to compare and identify the types of interactions such as hydrogen bonds, hydrophobic contacts, π-stacking, and cation-π interactions between ligand candidate-receptors and native ligand-receptors (Adasme *et al*., 2021). The physicochemical prediction of the ligands was conducted using the SwissADME website (http://www.swissadme.ch/index.php) (Daina *et al*., 2017).

Results and Discussion

Protein target

The crystal structure of the human protein $KRAS^{G12C}$ was used in this study as a protein target, with Sotorasib as the native ligand. Previously, Sotorasib was reported to form a covalent bond with cysteine-12 in the $KRAS^{G12C}$ mutant (Canon et al., 2019). However, this study focuses exclusively on molecular docking for non-covalent interactions to efficiently screen compounds for their initial binding potential and identify promising leads for further exploration. To align with this focus, Sotorasib was modified into its non-covalently bound state before the molecular docking process, as shown in Figure 2. The protein target was then separated from the native ligand and redocked to validate the docking parameters. Validation was confirmed by

the root mean square deviation (RMSD), which was calculated as 0.541 Å (< 2 Å), demonstrating the reliability of the docking procedure.

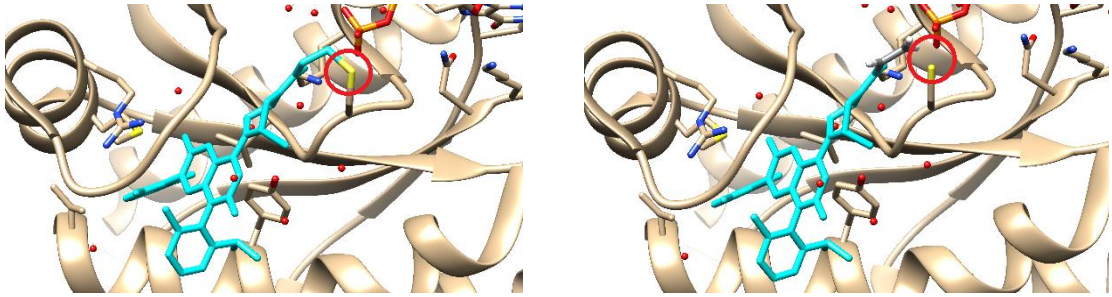

(a) (b)

Figure 2. Binding interactions of Sotorasib (shown in cyan) with $KRAS^{G12C}$, (a) covalently bound state (shown in red circle) with cysteine (b) non-covalently bound state

Virtual screening

Virtual screening was conducted on 218 compounds reported from *M. oleifera* with the first screening performed to evaluate the drug-likeness of the compounds using the combination of Lipinski's rule of five (MW ≤ 500), Ghose's rule (MW 160 ≤ MW ≤ 480) and Veber's rule (the polar surface area ≤ 140 Å and the number of rotatable bonds ≤ 10) (Ghose *et al*., 1999; Lipinski, 2001; Veber *et al*., 2002). The virtual screening results showed 74 compounds met the combined criteria. The compounds were then ranked based on the binding affinity values and 10 compounds with the lowest values were selected for further analysis. Binding affinity is often expressed as Gibbs free energy (ΔG) which quantifies the stability of the ligand-receptor complex. A lower ΔG indicates a spontaneous and thermodynamically favorable binding process. This will cause stronger and more favorable interactions that make the ligand bind tightly to the receptor (Du *et al*., 2016). The structure of the top ten compounds is shown in Figure 3.

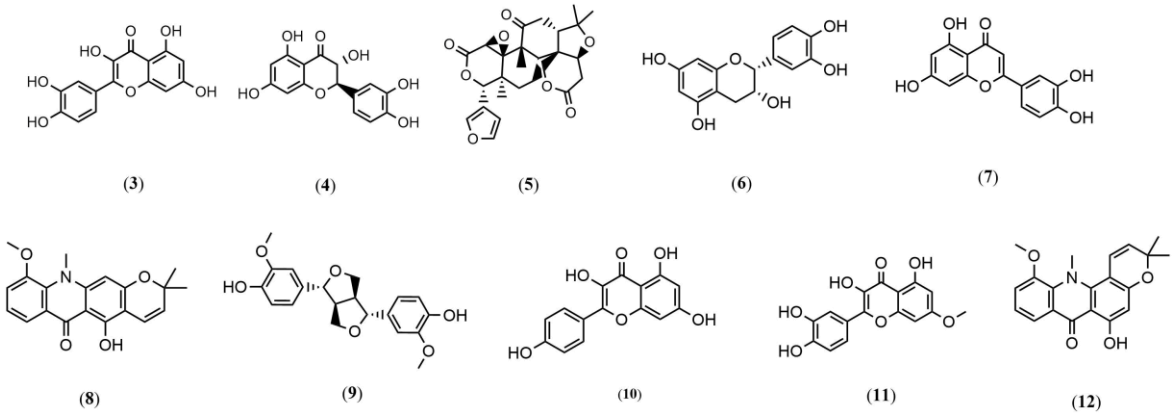

Figure 3. The top 10 compounds were isolated from *M. oleifera* that pass the drug-likeness criteria and have the lowest binding affinity viz. Quercetin (**3**), Dihydroquercetin (**4**), (1R,2R,7S,10S,13R,14R,16S,19S,20S)-19-(furan-3-yl)-9,9,13,20-tetramethyl-4,8,15,18-tetraoxahexacyclo[11.9.0.02,7.02,10.014,16.014,20]docosane-5,12,17-trione (**5**), Epicatechin (**6**), Luteolin (**7**), 5-hydroxy-10-methoxy-2,2,11-trimethylpyrano[3,2-b]acridin-6-one (**8**), Pinoresinol (**9**), Kaempferol (**10**), Rhamnaetin (**11**), 5-Methoxynoracronycine (**12**)

The screening results indicate that compound (**3)** (quercetin), has the lowest binding affinity value of -9.37179 kcal/mol. It is followed by compound (**4)** (dihydroquercetin) and compound (**5)** with the binding affinity value of -9.03297 kcal/mol and -8.91905 kcal/mol, respectively. The native ligand (Sotorasib) has a binding affinity of -10.2 kcal/mol. Although the binding affinities values of these compounds are slightly higher than that of the native ligand, they still exhibit strong interactions with the target protein, suggesting that they have potential as $KRAS^{G12C}$ inhibitors. The list of the binding affinity values of the top ten compounds is shown in Table 1.

Table 1. Analysis of interactions and the amino acid residue parts involved in the interactions using PLIP.

Compounds	Binding affinity (kcal/mol)	Type of interaction	Residue
Sotorasib (1)	-10.2	Hydrophobic interaction	PRO35A, GLU64A, HIS96A, TYR97A, TYR97A, GLN100A GLN100A, VAL104A
		H-bond	LYS17A, GLU64A
		Π-stacking	TYR97A, TYR97A
Quercetin (3)	-9.37179	Hydrophobic interaction	GLN100A, VAL104A
		H-bond	LYS17A, THR59A, GLY61A, ARG69A, ARG69A, GLN100A
		Π-stacking	TYR97A
		Cation-Π interactions	ARG69A
Dihydroquercetin (4)	-9.03297	Hydrophobic interaction	VAL10A, THR59A, TYR97A, GLN100A
		H-bond	THR59A, GLU63A, ARG69A, ARG69A, TYR97A
		Π-stacking	TYR97A
(1R,2R,7S,10S,13R,14R,16S,19S,20S)-19-(furan-3-yl)-9,9,13,20-tetramethyl-4,8,15,18-tetraoxahexacyclo[11.9.0.02,7.02,10.014,16.014,20]docosane-5,12,17-trione (5)	-8.91905	Hydrophobic interaction	TYR97A, TYR97A, GLN100A, GLN100A
		H-bond	ARG69A
		Salt bridges	ARG69A
Epicatechin (6)	-8.88955	Hydrophobic interaction	VAL104A
		H-bond	GLY11A, GLY11A, LYS17A, THR59A, TYR97A
		Π-stacking	TYR97A

Luteolin (7)	-8.79014	Hydrophobic interaction	GLN100A, VAL104A
		H-bond	LYS17A, THR59A, GLU64A, ARG69A, GLN100A
		Π-stacking	TYR97A
		Cation-Π interactions	ARG69A
5-hydroxy-10-methoxy-2,2,11-trimethylpyrano[3,2-b]acridin-6-one (8)	-8.65297	Hydrophobic interaction	VAL10A, GLN62A, TYR97A, GLN100A
		H-bond	LYS17A, THR59A
		Π-stacking	TYR97A
		Cation-Π interactions	ARG69A
Pinoresinol (9)	-8.60571	Hydrophobic interaction	VAL10A, HIS96A, TYR97A, TYR97A
		H-bond	ARG69A, ARG69A, ASP93A
Kaempferol (10)	-8.46609	Hydrophobic interaction	TYR97A, TYR97A, GLN100A
		H-bond	LYS17A, GLN62A, ARG69A, ARG69A
		Cation-Π interactions	ARG69A
Rhamnetin (11)	-8.34927	Hydrophobic interaction	GLN100A
		H-bond	LYS17A, GLY61A, ARG69A, GLN100A
5-Methoxynoracronycine (12)	-8.30672	Hydrophobic interaction	VAL10A, THR59A, GLU64A, TYR97A
		H-bond	TYR97A

In addition to binding affinity, the interactions between the ligands and $KRAS^{G12C}$ were also analyzed. Using the PLIP website, the interaction of the native ligand Sotorasib with $KRAS^{G12C}$ revealed several key interactions, including hydrophobic interactions with residues GLU64A, HIS96A, TYR97A, GLN100A, and VAL104A; hydrogen bonds with LYS17A and GLU64A; and π-stacking with TYR97A.

The top three ligands, compound (**3)** (quercetin), (**4)** (dihydroquercetin), and compound (**5)**, showed interactions with key residues. Quercetin, for example, exhibited similar interactions to Sotorasib, including two hydrophobic interactions with GLN100A and VAL104A, one hydrogen bond with LYS17A, and the same π-stacking with TYR97A. Dihydroquercetin also formed hydrophobic interactions with TYR97A and GLN100A and π-stacking with TYR97A as well. Compound (**5)** also showed hydrophobic interaction with TYR97A and GLN100A. The interaction of these compounds with key residues indicates that the three compounds might have a comparable binding mechanism to their native ligand and could potentially target the $KRAS^{G12C}$ protein effectively. The visualization of the interaction is shown in Figure 4.

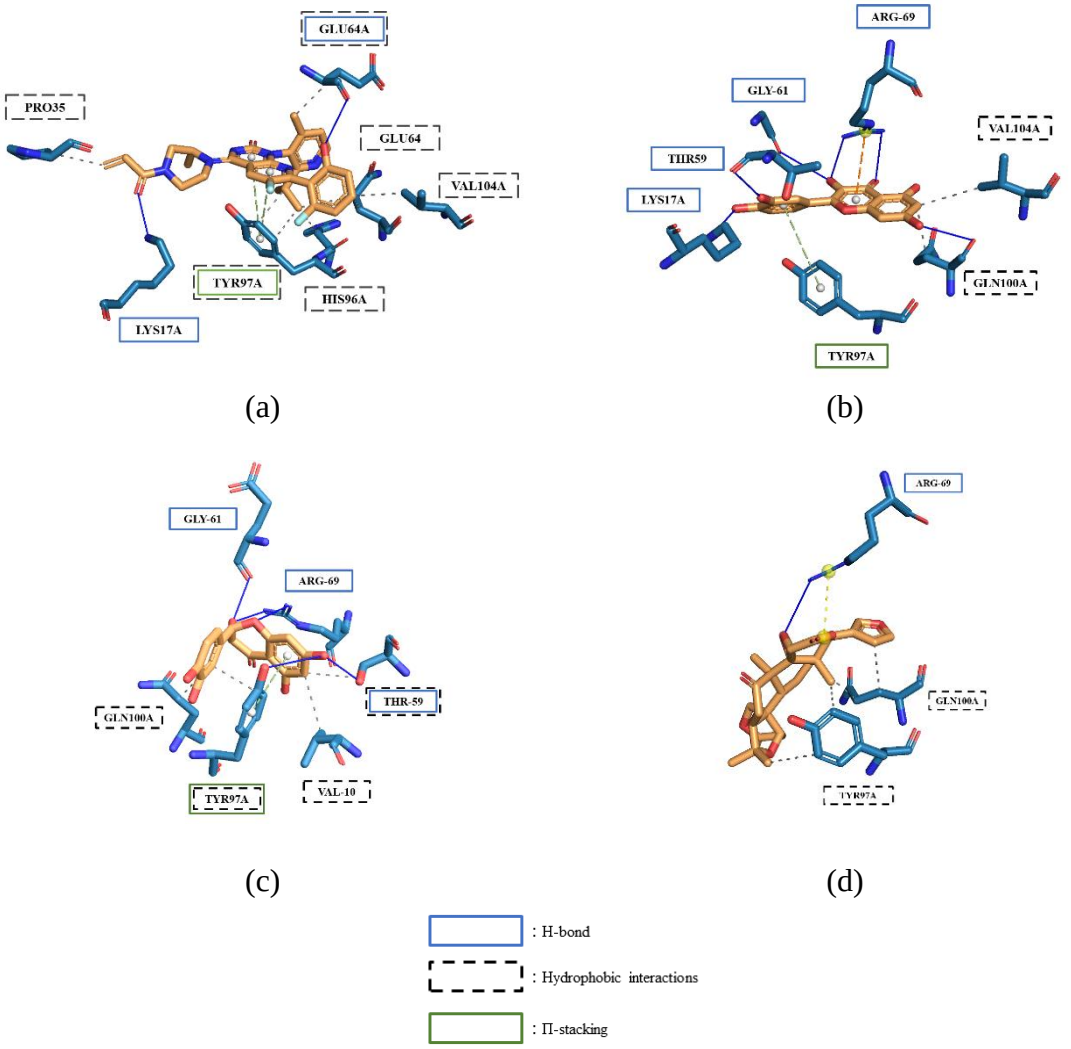

Figure 4. Molecular interactions between the $KRAS^{G12C}$ protein and (a) Sotorasib (**1**), (b) Quercetin (**3**), (c) Dihydroquercetin (**4**), and (d) Compound (**5)**

Physicochemical analysis

Computational methods for predicting physicochemical properties offer an effective alternative to experimental procedures in living organisms. The SMILES of the top 10 compounds from molecular docking were input into the SwissADME database to assess various parameters, including molecular weight, lipophilicity, pharmacokinetics, drug-likeness, and lead-likeness (Daina *et al*., 2017). The Physicochemical analysis results are presented in Table 2.

Based on the Physicochemical analysis, all ligands derived from *Moringa oleifera* exhibited good lipophilicity shown by the consensus LogP (the average of the LogP values predicted by the five methods used in SwissADME), for the top three rank ligands, the value is <5 means that it has good lipophilicity. The prediction also showed that all the top ten rank compounds have a high gastrointestinal value, making it a good candidate for colorectal cancer treatment. In addition to the Lipinski, Ghose and Veber rule, which has been used to predict the drug-likeness criteria for the virtual screening, the SwissADME prediction also shows prediction based on Egan and Muegge's prediction. All of the 10 compounds show drug-likeness based on these two predictions. It also gives an Abbot

bioavailability score (Martin, 2005) of 0.55, meaning that the compounds have a good drug-likeness score. Based on the lead likeness by Teague (Teague *et al*., 1999), most of the compounds showed lead-like properties meaning it's easy for them to go under chemical modification, except for compounds (**5)** and (**9)** which have molecular weights > 350 g/mol and compounds (**8)** and (**12)** which are highly lipophilic (XLOGP3>3.5).

Table 2. Physicochemical analysis of top ten rank *M. oleifera* compounds

Compound	MW (gram/mol)	Lipophilicity	Pharmaco-kinetics	Druglikeness			Medicinal Chemistry
		Consensus Log $P_{o/w}$	GI absorption	Egan	Muegge	Bio-availability Score	Lead-likeness
3	297.196	1.23	High	Yes	Yes	0.55	Yes
4	297.196	0.51	High	Yes	Yes	0.55	Yes
5	440.273	2.54	High	Yes	Yes	0.55	No; 1 violation: MW>350
6	281.197	0.85	High	Yes	Yes	0.55	Yes
7	280.189	1.73	High	Yes	Yes	0.55	Yes
8	319.226	3.33	High	Yes	Yes	0.55	No; 1 violation: XLOGP3>3.5
9	338.226	2.26	High	Yes	Yes	0.55	No; 1 violation: MW>350
10	280.189	1.86	High	Yes	Yes	0.55	Yes
11	308.199	1.63	High	Yes	Yes	0.55	Yes
12	319.226	3.25	High	Yes	Yes	0.55	No; 1 violation: XLOGP3>3.5

The virtual screening of 218 *Moringa oleifera* compounds identified 74 compounds that met drug-likeness criteria based on Lipinski's, Ghose's, and Veber's rules. Quercetin (**3**) (-9.37 kcal/mol), dihydroquercetin (**4**) (-9.03 kcal/mol), and compound (**5)** (-8.92 kcal/mol) emerged as the top candidates based on their binding affinity, which was comparable to the native ligand Sotorasib (**1**) (-10.2 kcal/mol). Interaction analysis revealed that these compounds engage with key KRASG12C active site residues, including GLN100A, VAL104A, LYS17A, and TYR97A, through hydrophobic interactions, hydrogen bonding, and π-stacking, suggesting a similar binding mechanism to Sotorasib. The physicochemical analysis further supported these findings, with the top compounds exhibiting good lipophilicity (LogP<5), high gastrointestinal absorption, and favorable bioavailability scores (Abbott score 0.55). Most of the compounds also showed lead-like properties.

In addition to its strong binding affinity, quercetin (**1**) has been previously reported to induce apoptosis in KRAS-mutant colorectal cancer cells, including $KRAS^{G13D}$, by activating the JNK pathway and inhibiting the AKT pathway (Yang *et al*., 2019). Activation of the JNK pathway is crucial for apoptosis, as blocking JNK activity prevents cell death in KRAS-mutant cells treated with quercetin. These findings support quercetin's potential as an anticancer agent for targeting KRAS mutations in colorectal cancer (Roni *et al*., 2021) However, since this study only investigated non-covalent interactions, future research should explore quercetin derivatives with functional groups

capable of forming covalent bonds with the cysteine residue of $KRAS^{G12C}$, similar to inhibitors like ARS-853 and ARS-1620. These covalent inhibitors have been shown to bind specifically to the active site of $KRAS^{G12C}$ and improve therapeutic potential in both *in vitro* and *in vivo* models (Hansen *et al*., 2018). The research highlights the potential of *Moringa oleifera* compounds, particularly quercetin (**3**), as promising inhibitors of $KRAS^{G12C}$. Their favorable binding profiles, ability to interact with key residues, and previously reported apoptotic effects in KRAS-mutant cells suggest they may serve as a basis for developing novel therapeutic agents for colorectal cancer.

Conclusions

In conclusion, this study suggests that bioactive compounds from *Moringa oleifera* leaves, particularly quercetin (**3**), show potential as inhibitors of $KRAS^{G12C}$ in colorectal cancer. This is supported by their low binding affinity and key interactions that are similar to native ligands, including hydrophobic interactions (GLN100A, VAL104A), hydrogen bonds (LYS17A, GLN100A), and π-stacking (TYR97A). Nevertheless, further studies, such as covalent docking and experimental validation, are necessary to confirm these findings.

Acknowledgment

We would like to thank the Bioinformatics Laboratory, Research Center for Biomolecule Engineering (BIOME) Universitas Airlangga, for providing the computational server used for the docking analysis in this study.

Conflict of Interest

The authors declare no conflict of interest.

References

Adasme, M. F., Linnemann, K. L., Bolz, S. N., Kaiser, F., Salentin, S., Haupt, V. J., and Schroeder, M., 2021. PLIP 2021: Expanding the scope of the protein–ligand interaction profiler to DNA and RNA. *Nucleic Acids Research*, 49(W1), W530–W534.

Aja, P. M., Agu, P. C., Ezeh, E. M., Awoke, J. N., Ogwoni, H. A., Deusdedit, T., Ekpono, E. U., Igwenyi, I. O., Alum, E. U., and Ugwuja, E. I., 2021. Prospect into therapeutic potentials of Moringa oleifera phytocompounds against cancer upsurge: De novo synthesis of test compounds, molecular docking, and ADMET studies. *Bulletin of the National Research Centre*, 45(1), 99.

Bell, E. W., and Zhang, Y., 2019. DockRMSD: an open-source tool for atom mapping and RMSD calculation of symmetric molecules through graph isomorphism. *Journal of Cheminformatics*, 11, 1–9.

Canon, J., Rex, K., Saiki, A. Y., Mohr, C., Cooke, K., Bagal, D., Gaida, K., Holt, T., Knutson, C. G., Koppada, N., Lanman, B. A., Werner, J., Rapaport, A. S., San Miguel, T., Ortiz, R., Osgood, T., Sun, J.-R., Zhu, X., McCarter, J. D., Volak, L. P., Houk, B. E., Fakih, M. G., O'Neil, B. H., Price, T. J., Falchook, G. S., Desai, J., Kuo, J., Govindan, R., Hong, D. S., Ouyang, W., Henary, H., Arvedson, T., Cee, V. J., and Lipford, J. R., 2019., The clinical KRAS(G12C) inhibitor AMG 510 drives anti-tumour immunity. *Nature*, 575(7781), 217–223.

Castro-González, L. M., Alvarez-Idaboy, J. R., and Galano, A., 2020. Computationally designed sesamol derivatives proposed as potent antioxidants. *ACS Omega*, 5(16), 9566–9575.

Cully, M., and Downward, J., 2008. SnapShot: Ras Signaling. *Cell*, 133(7), 1292-1292.e1.

Da Fonseca, A. M., Caluaco, B. J., Madureira, J. M. C., Cabongo, S. Q., Gaieta, E. M., Djata, F., Colares, R.

P., Neto, M. M., Fernandes, C. F. C., Marinho, G. S., Dos Santos, H. S., and Marinho, E. S. 2024. Screening of Potential Inhibitors Targeting the Main Protease Structure of SARS-CoV-2 via Molecular Docking, and Approach with Molecular Dynamics, RMSD, RMSF, H-Bond, SASA and MMGBSA. *Molecular Biotechnology*, 66(8), 1919–1933.

Daina, A., Michielin, O., and Zoete, V., 2017. SwissADME: a free web tool to evaluate pharmacokinetics, drug-likeness and medicinal chemistry friendliness of small molecules. *Scientific Reports*, 7(1), 42717.

Du, X., Li, Y., Xia, Y.-L., Ai, S.-M., Liang, J., Sang, P., Ji, X.-L., and Liu, S.-Q., 2016. Insights into protein–ligand interactions: Mechanisms, models, and methods. *International Journal of Molecular Sciences*, 17(2), 144.

Ferlay, J., Colombet, M., Soerjomataram, I., Parkin, D. M., Piñeros, M., Znaor, A., and Bray, F., 2021. Cancer statistics for the year 2020: An overview. *International Journal of Cancer*, 149(4), 778–789.

Ghose, A. K., Viswanadhan, V. N., and Wendoloski, J. J., 1999. A knowledge-based approach in designing combinatorial or medicinal chemistry libraries for drug discovery. 1. A qualitative and quantitative characterization of known drug databases. *Journal of Combinatorial Chemistry*, 1(1), 55–68.

Giannakis, M., Mu, X. J., Shukla, S. A., Qian, Z. R., Cohen, O., Nishihara, R., Bahl, S., Cao, Y., Amin-Mansour, A., Yamauchi, M., Sukawa, Y., Stewart, C., Rosenberg, M., Mima, K., Inamura, K., Nosho, K., Nowak, J. A., Lawrence, M. S., Giovannucci, E. L., Chan, A. T., Ng, K., Meyerhardt, J. A., Van Allen, E. M., Getz, G., Gabriel, S. B., Lander, E. S., Wu, C. J., Fuchs, C. S., Ogino, S., and Garraway, L. A., 2016. Genomic Correlates of Immune-Cell Infiltrates in Colorectal Carcinoma. *Cell Reports*, 15(4), 857–865.

Hansen, R., Peters, U., Babbar, A., Chen, Y., Feng, J., Janes, M. R., Li, L.-S., Ren, P., Liu, Y., and Zarrinkar, P. P., 2018. The reactivity-driven biochemical mechanism of covalent KRASG12C inhibitors. *Nature Structural and Molecular Biology*, 25(6), 454–462.

Hobbs, G. A., Wittinghofer, A., and Der, C. J., 2016. Selective Targeting of the KRAS G12C Mutant: Kicking KRAS When It's Down. *Cancer Cell*, 29(3), 251–253.

Huang, L., Guo, Z., Wang, F., and Fu, L., 2021. KRAS mutation: From undruggable to druggable in cancer. *Signal Transduction and Targeted Therapy*, 6(1), 386.

Jänne, P. A., Riely, G. J., Gadgeel, S. M., Heist, R. S., Ou, S.-H. I., Pacheco, J. M., Johnson, M. L., Sabari, J. K., Leventakos, K., Yau, E., Bazhenova, L., Negrao, M. V., Pennell, N. A., Zhang, J., Anderes, K., Der-Torossian, H., Kheoh, T., Velastegui, K., Yan, X., Christensen, J. G., Chao, R. C., and Spira, A. I., 2022. Adagrasib in Non–Small-Cell Lung Cancer Harboring a KRASG12C Mutation. *New England Journal of Medicine*, 387(2), 120–131.

Kashyap, P., Kumar, S., Riar, C. S., Jindal, N., Baniwal, P., Guiné, R. P. F., Correia, P. M. R., Mehra, R., and Kumar, H., 2022. Recent advances in Drumstick (Moringa oleifera) leaves bioactive compounds: Composition, health benefits, bioaccessibility, and dietary applications. *Antioxidants*, 11(2), 402.

Koes, D. R., Baumgartner, M. P., and Camacho, C. J., 2013. Lessons Learned in Empirical Scoring with smina from the CSAR 2011 Benchmarking Exercise. *Journal of*

Chemical Information and Modeling, 53(8), 1893–1904.

Kontoyianni, M., 2017. Docking and Virtual Screening in Drug Discovery. In I. M. Lazar, M. Kontoyianni, and A. C. Lazar (Eds.), *Proteomics for Drug Discovery*, 1647, 255–266.

Lin, M., Zhang, J., and Chen, X., 2018. Bioactive flavonoids in *Moringa oleifera* and their health-promoting properties. *Journal of Functional Foods*, 47, 469–479.

Lipinski, C. A., 2001. Avoiding investment in doomed drugs. *Curr Drug Discov*, 1, 17–19.

Martin, Y. C., 2005. A bioavailability score. *Journal of Medicinal Chemistry*, 48(9), 3164–3170.

Milburn, M. V., Tong, L., Devos, A. M., Brunger, A., Yamaizumi, Z., Nishimura, S., and Kim, S.-H., 1990. *Molecular Switch for Signal Transduction*, 247.

Mthiyane, F. T., Dludla, P. V., Ziqubu, K., Mthembu, S. X. H., Muvhulawa, N., Hlengwa, N., Nkambule, B. B., and Mazibuko-Mbeje, S. E., 2022. A Review on the Antidiabetic Properties of Moringa oleifera Extracts: Focusing on Oxidative Stress and Inflammation as Main Therapeutic Targets. *Frontiers in Pharmacology*, 13, 940572.

Mumtaz, M. Z., Kausar, F., Hassan, M., Javaid, S., and Malik, A., 2021. Anticancer activities of phenolic compounds from Moringa oleifera leaves: In vitro and in silico mechanistic study. *Beni-Suef University Journal of Basic and Applied Sciences*, 10(1), 12.

Neumann, J., Zeindl-Eberhart, E., Kirchner, T., and Jung, A., 2009. Frequency and type of KRAS mutations in routine diagnostic analysis of metastatic colorectal cancer. *Pathology - Research and Practice*, 205(12), 858–862.

O'Boyle, N. M., Banck, M., James, C. A., Morley, C., Vandermeersch, T., and Hutchison, G. R., 2011. Open Babel: An open chemical toolbox. *Journal of Cheminformatics*, 3(1), 33.

Parikh, K., Banna, G., Liu, S. V., Friedlaender, A., Desai, A., Subbiah, V., and Addeo, A., 2022. Drugging KRAS: Current perspectives and state-of-art review. *Journal of Hematology and Oncology*, 15(1), 152.

Pettersen, E. F., Goddard, T. D., Huang, C. C., Couch, G. S., Greenblatt, D. M., Meng, E. C., and Ferrin, T. E., 2004. UCSF Chimera—A visualization system for exploratory research and analysis. *Journal of Computational Chemistry*, 25(13), 1605–1612.

Puranen, J. S., Vainio, M. J., and Johnson, M. S., 2010. Accurate conformation-dependent molecular electrostatic potentials for high-throughput in silico drug discovery. *Journal of Computational Chemistry*, 31(8), 1722–1732.

Roni, A., Maruf, A., and Marliani, L., 2021. Uji Sitotoksik Ekstrak Tanaman Gandaria (*Bouea macrophylla* Griff) terhadap Sel HeLa. *Jurnal Kimia Riset*, 6(1), 39.

Sahakitpichan, P., Mahidol, C., Disadee, W., Ruchirawat, S., and Kanchanapoom, T., 2011. Unusual glycosides of pyrrole alkaloid and 4′-hydroxyphenylethanamide from leaves of *Moringa oleifera*. *Phytochemistry*, 72(8), 791–795.

Schrodinger., 2015. *The PyMOL Molecular Graphics System, Version 1.8*.

Sharma, V., and Paliwal, R., 2014. Potential Chemoprevention of 7,12-Dimethylbenz[a]anthracene Induced Renal Carcinogenesis by Moringa oleifera Pods and Its Isolated Saponin. *Indian Journal of Clinical Biochemistry*, 29(2), 202–209.

Simanshu, D. K., Nissley, D. V., and McCormick, F., 2017. RAS Proteins

and Their Regulators in Human Disease. *Cell*, 170(1), 17–33.

Sivani, B. M., Venkatesh, P., Murthy, T. P. K., and Kumar, S. B., 2021. In silico screening of antiviral compounds from Moringa oleifera for inhibition of SARS-CoV-2 main protease. *Current Research in Green and Sustainable Chemistry*, 4, 100202.

Teague, S. J., Davis, A. M., Leeson, P. D., and Oprea, T., 1999. The Design of Leadlike Combinatorial Libraries. *Angewandte Chemie International Edition*, 38(24), 3743–3748.

Teclegeorgish, Z. W., Aphane, Y. M., Mokgalaka, N. S., Steenkamp, P., and Tembu, V. J., 2021. Nutrients, secondary metabolites and anti-oxidant activity of Moringa oleifera leaves and Moringa-based commercial products. *South African Journal of Botany*, 142, 409–420.

Tukiran, Miranti, M. G., Dianawati, I., and Sabila, F. I., 2020. Aktivitas Antioksidan Ekstrak Daun Kelor (Moringa oleifera Lam.) dan Buah Bit (Beta vulgaris L.) sebagai Bahan Tambahan Minuman Suplemen. *Jurnal Kimia Riset*, 5(2), 113.

Veber, D. F., Johnson, S. R., Cheng, H.-Y., Smith, B. R., Ward, K. W., and Kopple, K. D., 2002. Molecular properties that influence the oral bioavailability of drug candidates. *Journal of Medicinal Chemistry*, 45(12), 2615–2623.

Waterman, C., Cheng, D. M., Rojas-Silva, P., Poulev, A., Dreifus, J., Lila, M. A., and Raskin, I., 2014. Stable, water extractable isothiocyanates from *Moringa oleifera* leaves attenuate inflammation *in vitro*. *Phytochemistry*, 103, 114–122.

Xie, J., Peng, L., Yang, M., Jiang, W., Mao, J., Shi, C., Tian, Y., and Sheng, J., 2021. Alkaloid Extract of Moringa oleifera Lam. Exerts Antitumor Activity in Human Non-Small-Cell Lung Cancer via Modulation of the JAK2/STAT3 Signaling Pathway. *Evidence-Based Complementary and Alternative Medicine*, 2021(1), 5591687.

Yaeger, R., Chatila, W. K., Lipsyc, M. D., Hechtman, J. F., Cercek, A., Sanchez-Vega, F., Jayakumaran, G., Middha, S., Zehir, A., Donoghue, M. T. A., You, D., Viale, A., Kemeny, N., Segal, N. H., Stadler, Z. K., Varghese, A. M., Kundra, R., Gao, J., Syed, A., Hyman, D. M., Vakiani, E., Rosen, N., Taylor, B. S., Ladanyi, M., Berger, M. F., Solit, D. B., Shia, J., Saltz, L., and Schultz, N., 2018. Clinical Sequencing Defines the Genomic Landscape of Metastatic Colorectal Cancer. *Cancer Cell*, 33(1), 125-136.e3.

Yang, Y., Wang, T., Chen, D., Ma, Q., Zheng, Y., Liao, S., Wang, Y., and Zhang, J., 2019. Quercetin preferentially induces apoptosis in KRAS-mutant colorectal cancer cells via JNK signaling pathways. *Cell Biology International*, 43(2), 117–124.

Zhao, H., Yang, Y., Wang, S., Yang, X., Zhou, K., Xu, C., Zhang, X., Fan, J., Hou, D., and Li, X., 2023. NPASS database update 2023: Quantitative natural product activity and species source database for biomedical research. *Nucleic Acids Research*, 51(D1), D621–D628.